

## SUPPLEMENTARY INFORMATION

### **$\text{XB}_2\text{Bi}_2$ ( $\text{X} = \text{Si, Ge, Sn, Pb}$ ): Penta-atomic Planar Tetracoordinate Si/Ge/Sn/Pb Clusters with 20 Valence Electrons**

Yan-Xia Jin and Jin-Chang Guo\*

*Key Laboratory of Materials for Energy Conversion and Storage of Shanxi Province, Institute of Molecular Science, Shanxi University, Taiyuan, Shanxi 030006, China.*

E-mail: guojc@sxu.edu.cn

#### Table of Contents

- Table S1.** Cartesian coordinates of optimized structures of the **1–4E** in the text.
- Table S2.** Orbital composition analysis of canonical molecular orbitals (CMOs) of the global-minimum structure **1** ( $C_{2v}$ ,  $^1\text{A}_1$ ) of  $\text{SiB}_2\text{Bi}_2$  cluster.
- Figure S1.** Optimized GM structures of  $\text{XB}_2\text{Bi}_2$  ( $\text{X} = \text{Si, Ge, Sn, Pb}$ ) clusters with bond distances (in Å) at the MP2/def2-TZVP level. The lowest vibrational frequencies are shown (in  $\text{cm}^{-1}$ ).
- Figure S2.** HOMO, LUMO, and HOMO–LUMO gap values of  $\text{XB}_2\text{Bi}_2$  ( $\text{X} = \text{Si, Ge, Sn, Pb}$ ) at the PBE0-D3(BJ)/def2-TZVP level. Those of ptC  $\text{CB}_2\text{Bi}_2$  are also listed.
- Figure S3.** ELF $_{\sigma}$  (a) and ELF $_{\pi}$  (b) pictures of ptSi  $\text{SiB}_2\text{Bi}_2$ .
- Figure S4.** Color-filled maps of (a) ICSS(0) $_{zz}$  and (b) ICSS(1) $_{zz}$  (in ppm) for **2–4** clusters. Positive values indicate aromaticity. 0 and 1 in parentheses represent the height above the molecular planes (in Å).
- Figure S5.** Simulated infrared spectra of **2–4** clusters at the PBE0-D3(BJ)/def2-TZVP level.

**Table S1.** Cartesian coordinates of optimized structures of the **1–4E** in the text.

**1 SiB<sub>2</sub>Bi<sub>2</sub>** ( $C_{2v}, ^1A_1$ )

Si	0. 00000000	0. 00000000	-0. 69264364
B	0. 00000000	0. 78509201	1. 24503740
B	0. 00000000	-0. 78509201	1. 24503740
Bi	0. 00000000	2. 55212806	-0. 01658652
Bi	0. 00000000	-2. 55212806	-0. 01658652

**1B** ( $C_s, ^1A'$ )

Si	-0. 94882408	1. 97728437	0. 00000000
B	0. 92192294	1. 42269341	0. 00000000
B	-0. 04654403	0. 08502439	0. 00000000
Bi	2. 34380697	-0. 15531056	0. 00000000
Bi	-2. 23649803	-0. 26903366	0. 00000000

**1C** ( $C_s, ^1A'$ )

Si	0. 49035137	2. 04064972	0. 00000000
B	-1. 70690907	0. 06829469	0. 00000000
B	-1. 40945243	1. 62902767	0. 00000000
Bi	0. 05251138	-0. 22322716	1. 51142293
Bi	0. 05251138	-0. 22322716	-1. 51142293

**1D** ( $C_s, ^1A'$ )

Si	-3. 16275301	1. 39061380	0. 00000000
B	-1. 31584304	1. 82797793	0. 00000000
B	0. 25495699	1. 47664304	0. 00000000
Bi	-1. 27884787	-0. 53173907	0. 00000000
Bi	1. 87623308	0. 09810415	0. 00000000

**1E** ( $C_s, ^1\text{A}'$ )

Si	1. 43138892	2. 25199596	0. 00000000
B	0. 04388196	0. 89758792	0. 00000000
B	-0. 28310599	-0. 72127209	0. 00000000
Bi	-2. 27725401	-0. 05596116	0. 00000000
Bi	2. 05022600	-0. 33451502	0. 00000000

**2 GeB<sub>2</sub>Bi<sub>2</sub>** ( $C_{2v}, ^1\text{A}_1$ )

Ge	0. 00000000	0. 00000000	-0. 63270333
B	0. 00000000	0. 78509201	1. 30497771
B	0. 00000000	-0. 78509201	1. 30497771
Bi	0. 00000000	2. 55212806	0. 04335379
Bi	0. 00000000	-2. 55212806	0. 04335379

**2B** ( $C_s, ^1\text{A}'$ )

Ge	0. 18696613	1. 90797657	0. 00000000
B	-1. 71776546	-0. 34815627	0. 00000000
B	-1. 63805844	1. 23866907	0. 00000000
Bi	0. 06503737	-0. 39462539	1. 51142293
Bi	0. 06503737	-0. 39462539	-1. 51142293

**2C** ( $C_s, ^1\text{A}'$ )

Ge	0. 93697204	1. 75591295	0. 00000000
B	-0. 94708287	1. 28107631	0. 00000000
B	-0. 04008516	-0. 08643272	0. 00000000
Bi	-2. 42327565	-0. 22607460	0. 00000000
Bi	2. 12150137	-0. 52287037	0. 00000000

**2D** ( $C_s, ^1\text{A}'$ )

Ge	-3. 01359681	0. 93725895	0. 00000000
B	-1. 22760024	1. 57958290	0. 00000000
B	0. 37274913	1. 40715661	0. 00000000

Bi	-0.92542555	-0.76099895	0.00000000
Bi	2.13879125	0.21972204	0.00000000

### 2E ( $C_s, ^1\text{A}'$ )

Ge	1.46438183	1.94856347	0.00000000
B	-0.02479150	0.70680685	0.00000000
B	-0.47737378	-0.88152502	0.00000000
Bi	-2.41338736	-0.06230811	0.00000000
Bi	1.87905734	-0.67842009	0.00000000

### 3 SnB<sub>2</sub>Bi<sub>2</sub> ( $C_{2v}, ^1\text{A}_1$ )

Sn	0.00000000	0.00000000	1.24128239
B	0.00000000	0.79608423	-1.24018059
B	0.00000000	-0.79608423	-1.24018059
Bi	0.00000000	2.69689122	-0.29917056
Bi	0.00000000	-2.69689122	-0.29917056

### 3B ( $C_s, ^1\text{A}'$ )

Sn	0.10781754	2.07980357	0.00000000
B	-1.65212270	-0.65341558	0.00000000
B	-1.90388277	0.91909968	0.00000000
Bi	0.07463344	-0.63444939	-1.51304437
Bi	0.07463344	-0.63444939	1.51304437

### 3C ( $C_s, ^1\text{A}'$ )

Sn	1.29054355	1.89424475	0.00000000
B	-0.10998643	-0.17542506	0.00000000
B	-1.03243961	1.17202512	0.00000000
Bi	1.91643704	-1.00275401	0.00000000
Bi	-2.62505207	-0.19839343	0.00000000

**3D** ( $C_1, ^1\text{A}$ )

Sn	1. 86824000	-0. 02450800	-0. 06553900
B	-0. 57684400	-0. 53949200	1. 94660500
B	0. 46808700	0. 62735800	1. 67857000
Bi	-0. 91073800	1. 48914100	-0. 07692100
Bi	-0. 92844200	-1. 47022100	-0. 07671300

**3E** ( $C_s, ^1\text{A}'$ )

Sn	3. 15910817	-0. 63956441	0. 00000000
B	-0. 54578919	-1. 35498978	0. 00000000
B	1. 05753414	-1. 42686307	0. 00000000
Bi	-2. 43143113	-0. 33746760	0. 00000000
Bi	0. 49752590	0. 89032887	0. 00000000

**4 PbB<sub>2</sub>Bi<sub>2</sub>** ( $C_{2v}, ^1\text{A}_1$ )

Pb	0. 00000000	0. 00000000	1. 08732488
B	0. 00000000	0. 79608423	-1. 39413810
B	0. 00000000	-0. 79608423	-1. 39413810
Bi	0. 00000000	2. 69689122	-0. 45312807
Bi	0. 00000000	-2. 69689122	-0. 45312807

**4B** ( $C_s, ^1\text{A}'$ )

Pb	0. 06407749	1. 82316412	0. 00000000
B	-1. 65007956	-0. 93899848	0. 00000000
B	-1. 92800478	0. 62910386	0. 00000000
Bi	0. 07612089	-0. 89126497	-1. 51304437
Bi	0. 07612089	-0. 89126497	1. 51304437

**4C** ( $C_s, ^1\text{A}'$ )

Pb	1. 29928034	1. 53072606	0. 00000000
B	-0. 31185493	-0. 37957771	0. 00000000

B	-1.08695072	1.05770040	0.00000000
Bi	1.61593793	-1.41614898	0.00000000
Bi	-2.81529889	-0.13698536	0.00000000

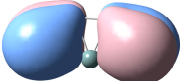
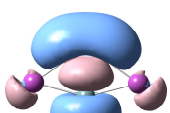
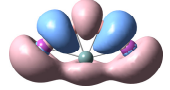
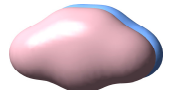
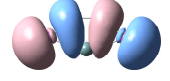
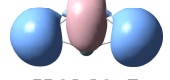
**4D ( $C_1, ^1\text{A}$ )**

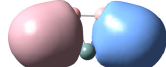
Pb	1.86824000	-0.02450800	-0.06553900
B	-0.57684400	-0.53949200	1.94660500
B	0.46808700	0.62735800	1.67857000
Bi	-0.91073800	1.48914100	-0.07692100
Bi	-0.92844200	-1.47022100	-0.07671300

**4E ( $C_s, ^1\text{A}'$ )**

Pb	-1.73452637	-1.38043592	0.00000000
B	0.32297867	-0.35057301	0.00000000
B	1.12268273	1.08967496	0.00000000
Bi	-1.14601025	1.55419306	0.00000000
Bi	2.77255068	-0.23491311	0.00000000

**Table S2.** Orbital composition analysis of canonical molecular orbitals (CMOs) of the global-minimum structure **1** ( $C_{2v}$ ,  $^1A_1$ ) of SiB<sub>2</sub>Bi<sub>2</sub> cluster.

CMO	Si (%)		B <sub>2</sub> (%)		Bi <sub>2</sub> (%)	
	s/p	total	s/p	total	s/p	total
 HOMO	0.00/0.00	0.00	0.00/13.87	13.87	0.00/ <b>84.68</b>	<b>84.68</b>
 HOMO-1	9.53/ <b>25.53</b>	<b>35.06</b>	9.30/ <b>45.55</b>	<b>54.85</b>	0.00/7.72	7.72
 HOMO-2	0.00/ <b>27.20</b>	<b>27.20</b>	4.72/ <b>15.90</b>	<b>20.62</b>	0.00/ <b>50.71</b>	<b>50.71</b>
 HOMO-3	1.87/5.58	7.45	0.00/ <b>42.34</b>	<b>42.34</b>	5.29/ <b>42.75</b>	<b>48.04</b>
 HOMO-4	0.00/ <b>26.65</b>	<b>26.65</b>	0.00/ <b>46.37</b>	<b>46.37</b>	0.00/ <b>25.53</b>	<b>25.53</b>
 HOMO-5	0.00/3.33	3.33	<b>19.69</b> /11.82	<b>31.51</b>	<b>18.63</b> / <b>44.16</b>	<b>62.79</b>
 HOMO-6	<b>41.02</b> /4.76	<b>45.78</b>	<b>21.40</b> /13.64	<b>35.04</b>	3.58/13.32	<b>16.90</b>
 HOMO-7	2.65/3.01	5.66	<b>15.31</b> / <b>27.25</b>	<b>42.56</b>	<b>43.23</b> /2.93	<b>46.16</b>

CMO	Si (%)		B <sub>2</sub> (%)		Bi <sub>2</sub> (%)	
	s/p	total	s/p	total	s/p	total
 HOMO-8	0.00/9.34	9.34	6.37/13.29	<b>19.66</b>	<b>63.42</b> /0.00	<b>63.42</b>
 HOMO-9	<b>16.83</b> /3.36	<b>20.19</b>	<b>26.04</b> /8.36	<b>34.40</b>	<b>34.51</b> /3.32	<b>37.83</b>

**Figure S1.** Optimized GM structures of  $\text{XB}_2\text{Bi}_2$  ( $\text{X} = \text{Si}, \text{Ge}, \text{Sn}, \text{Pb}$ ) clusters with bond distances (in Å) at the MP2/def2-TZVP level. The lowest vibrational frequencies are shown (in  $\text{cm}^{-1}$ ).

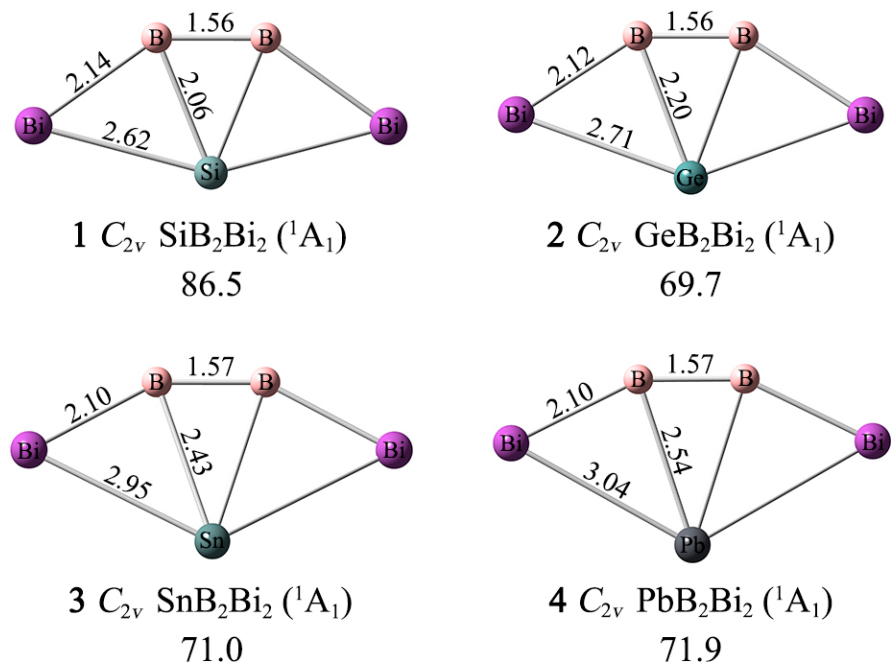


**Figure S2.** HOMO, LUMO, and HOMO–LUMO gap values of  $\text{XB}_2\text{Bi}_2$  ( $\text{X} = \text{Si}, \text{Ge}, \text{Sn}, \text{Pb}$ ) at the PBE0-D3(BJ)/def2-TZVP level. Those of ptC  $\text{CB}_2\text{Bi}_2$  are also listed.

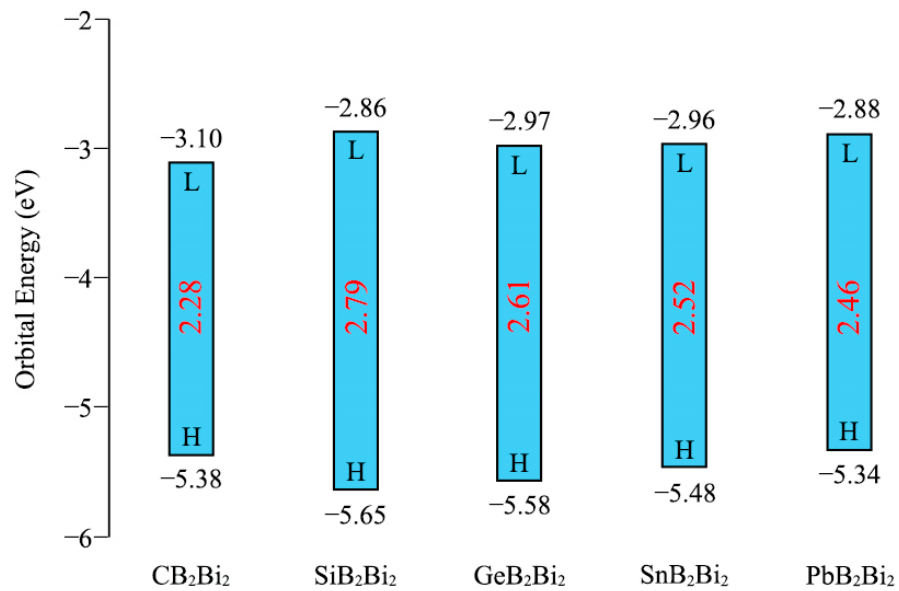


**Figure S3.** ELF<sub>σ</sub> (a) and ELF<sub>π</sub> (b) pictures of ptSi SiB<sub>2</sub>Bi<sub>2</sub>.

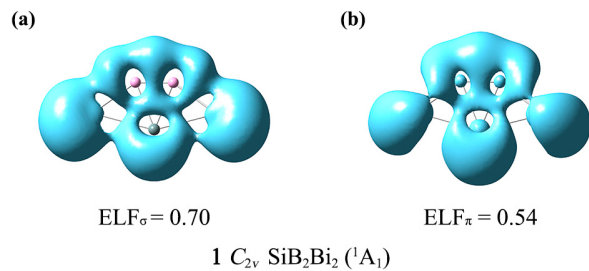


**Figure S4.** Color-filled maps of (a) ICSS(0)<sub>zz</sub> and (b) ICSS(1)<sub>zz</sub> (in ppm) for **2–4** clusters. Positive values indicate aromaticity. 0 and 1 in parentheses represent the height above the molecular planes (in Å).

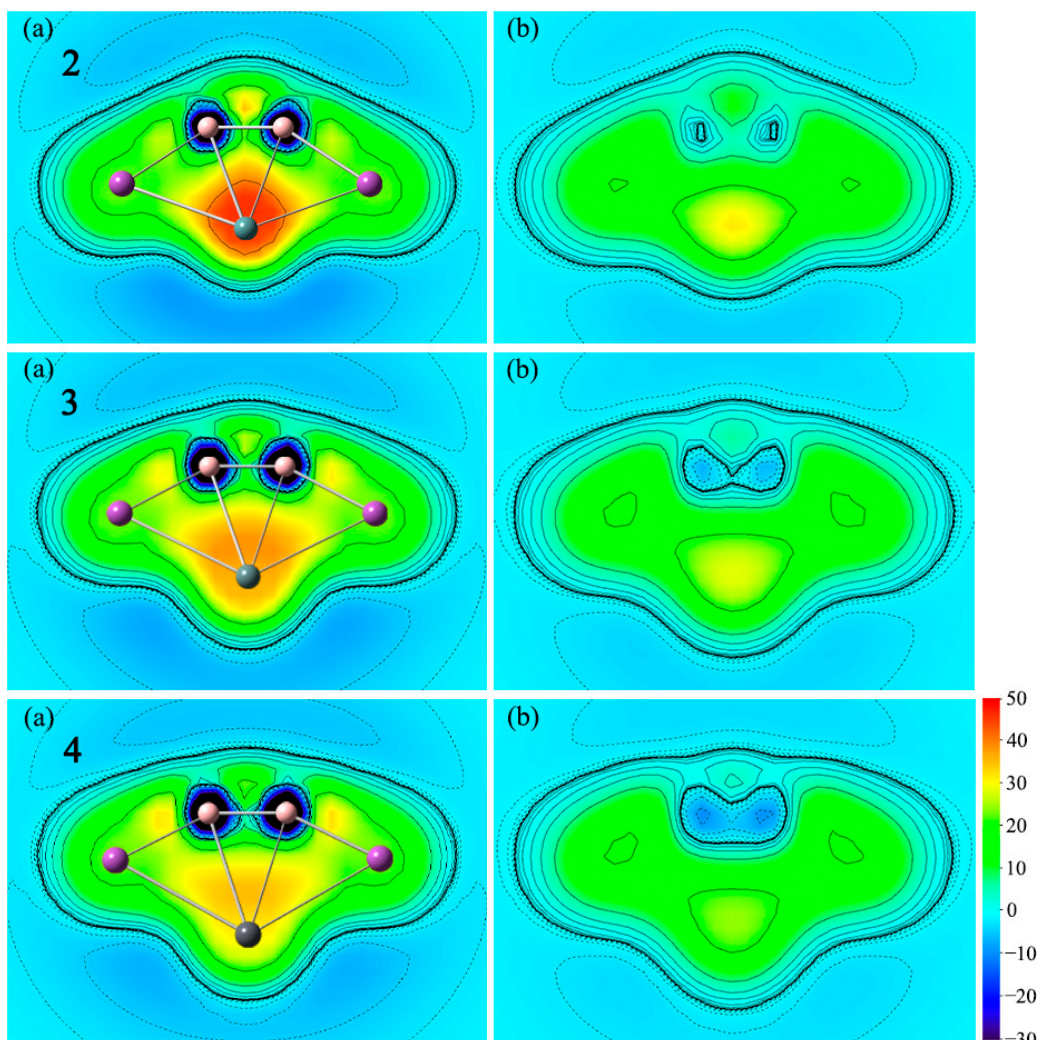


**Figure S5.** Simulated infrared spectra of **2–4** clusters at the PBE0-D3(BJ)/def2-TZVP level.

